

# Interactions between urbanization, heat stress, and climate change

K. W. Oleson · A. Monaghan · O. Wilhelmli ·  
M. Barlage · N. Brunzell · J. Feddema · L. Hu ·  
D. F. Steinhoff

Received: 22 January 2013 / Accepted: 8 September 2013  
© Springer Science+Business Media Dordrecht 2013

**Abstract** Heat stress (HS) is a leading cause of weather-related human mortality. As temperatures continue to increase due to climate change, HS is expected to worsen. HS can be magnified in urban areas because of the urban heat island effect. We use an urban canyon model coupled to a land surface model to quantify present-day and projected mid-21st century rural and urban HS for boreal summer over the U.S. and southern Canada and examine the effects of three urban density classes on HS. Five indices of HS are implemented in the model [the NWS Heat Index (HI), Apparent Temperature (AT), Simplified Wet Bulb Globe Temperature, Humidex, and Discomfort Index]. The present-day urban-rural contrast in HS differs according to which index is used. The HI and Humidex have higher urban-rural HS for all density classes than defined by temperature alone. Future urban HS is amplified by 0.5–1.0 °C for the AT, HI, and Humidex compared to temperature alone. For four cities examined in further detail, climate change by mid-century increases the number of high HS days and nights in both rural and urban areas, the magnitude being highly dependent on HS index, urban density class, and each city's climatic setting. Houston exhibits noteworthy mid-century increases in high heat stress nights, with more than half of summer nights qualifying as high HS in not only urban areas but also rural areas, indicating the need to consider vulnerability and adaptive capacity of both rural and urban populations in the context of climate change.

## 1 Introduction

Extreme heat events are a leading cause of weather-related human mortality in the U.S. and many countries world-wide (CDC 2006). High-risk groups such as the elderly, the very

---

This article is part of a Special Issue on “Regional Earth System Modeling” edited by Zong-Liang Yang and Congbin Fu.

**Electronic supplementary material** The online version of this article (doi:10.1007/s10584-013-0936-8) contains supplementary material, which is available to authorized users.

K. W. Oleson (✉) · A. Monaghan · O. Wilhelmli · M. Barlage · D. F. Steinhoff  
National Center for Atmospheric Research, P.O. Box 3000, Boulder, CO 80307, USA  
e-mail: oleson@ucar.edu

N. Brunzell · J. Feddema · L. Hu  
University of Kansas, 1475 Jayhawk Blvd, Lawrence, KS 66045, USA

young, individuals with health problems, and the urban poor are particularly susceptible to extreme heat events (Uejio et al. 2011). As climate continues to warm, extreme heat events are expected to worsen in severity (hotter days and nights), frequency (number of hot days and nights), and duration (heat waves) (Delworth et al. 1999; Meehl and Tebaldi 2004; IPCC 2007). In the absence of acclimatization, and adaptation and mitigation measures, human mortality due to extreme heat events can be expected to increase in a warming climate (IPCC 2007). Even acclimatization may not protect humans from unprecedented or intolerable heat stress under severe warming scenarios due to human physiological limits (Sherwood and Huber 2010).

In addition to global scale warming, extreme heat can be exacerbated in urban areas because of the urban heat island (UHI) effect (Stone 2012). Multiple local factors resulting from unique morphological, radiative, and thermal properties of urban areas are responsible for the UHI (Oke 1987; Oke et al. 1991). First, the urban canyon (Oke 1987) can decrease surface longwave radiation loss and increase absorption of solar radiation (lower albedo). Second, urban areas have reduced evapotranspiration due to replacement of vegetation with impervious surfaces. Third, urban surfaces generally store more sensible heat during the day that is then released at night. Fourth, anthropogenic heat emissions from vehicles, commercial and residential buildings, industry, and power plants also contribute directly to the heat island effect (Sailor 2010).

Analysis of extreme heat events has indicated a role of urban heat island effects in enhancing premature mortality and morbidity (e.g., Conti et al. 2005). Enhanced urban temperature, combined with urban effects on humidity, radiation, winds and air pollution all should be considered (Fischer et al. 2012). Furthermore, urban areas have a distinct asymmetry in their diurnal temperature cycle compared to rural areas, with the heat island being more pronounced at night than during the day. This characteristic of urban areas may exacerbate threats to human health due to heat stress because it deprives urban dwellers of the opportunity to cool off (Rogot et al. 1992).

Numerical modeling provides an opportunity to examine extreme heat events and heat stress in the context of climate change. Heat stress can be assessed in terms of temperature alone as is commonly done using climate models (Meehl and Tebaldi 2004), but it is recognized that humidity can aggravate the physiological effects of high temperature (Epstein and Moran 2006). In general, most indices of heat stress combine temperature and humidity but make assumptions about other factors that affect heat stress, such as radiation and wind speed, as well as human physiology and clothing (Epstein and Moran 2006). Several previous numerical modeling studies have examined changes in heat stress associated with climate change, however, few have considered the combined effects of temperature and humidity or urban areas explicitly (Delworth et al. 1999; Sherwood and Huber 2010; Diffenbaugh and Ashfaq 2010). Fischer et al. (2012) contrast the urban and rural heat stress response to a doubling of CO<sub>2</sub> using a land surface model including an urban canyon model [the Community Land Model (CLM) with CLM Urban (CLMU)] coupled to a global climate model (the Community Climate System Model (CCSM4); Gent et al. 2011). Heat stress was quantified with the Simplified Wet-Bulb Globe Temperature (SWBGT; Willett and Sherwood 2012). They found substantially higher heat stress in urban areas compared to rural areas, the contrast being most pronounced at night and over mid-latitudes and subtropics. Under doubled CO<sub>2</sub>, the occurrence of nights with extremely high heat stress increased more in urban than rural areas.

Here, we use CLM to quantify present-day (PD; 1986–2005) and a projection of one possible manifestation of mid-21st century (MC; 2046–2065) rural and urban heat stress for boreal summer over the U.S. and southern Canada at fine spatial resolution (1/8° in latitude and longitude) and examine the effects of urban density on heat stress. The Weather and

Research Forecasting model (WRF) is used to downscale a CCSM4 20th century ensemble member for PD and a CCSM4 RCP8.5 (representative concentration pathway; Moss et al. 2010) ensemble member for MC to provide a consistent set of atmospheric forcing variables for CLM (Section 2.2).

Fischer et al. (2012) used the dominant urban density type by area in their global analysis, which mainly represents medium density urban areas (Jackson et al. 2010). We expand this here by conducting PD and MC CLM simulations for three urban density classes available from the dataset of Jackson et al. (2010) [tall building district (TBD), high density (HD), and medium density (MD)] to explore the effects of urban density on heat stress (Section 2.3). The approach of Fischer et al. (2012) is also expanded to include additional indices of heat stress [Section 2.4 and Online Resource 1 (OR1)].

Present-day mean and diurnal cycle climatology of urban and rural heat stress for the three urban density classes are discussed in Section 3.1. In previous papers we have used global simulations to explore mean changes in the UHI under various future greenhouse gas scenarios (e.g., Oleson 2012). Here, we also focus on how urban density and a future greenhouse scenario produce changes in extreme heat events (Section 3.2).

## 2 Materials and methods

### 2.1 Community Land Model version 4 (CLM4) and CLM Urban (CLMU)

CLM4 (Lawrence et al. 2011) is the land surface model used in CCSM4. The land surface in CLM4 is described by subgrid fractions of landunits such as vegetation/soil (referred to here as rural surface) which consists of mixtures of plant functional types (PFTs) derived from satellite data as well as other landunits such as glaciers, wetlands, lakes, and urban.

The urban landunit consists of five components: roof, sunlit wall, shaded wall and a canyon floor subdivided into pervious (e.g., representing green space within the city) and impervious (e.g., representing roads, parking lots, sidewalks) fractions (CLMU; Oleson et al. 2008). The five urban components are arranged in an “urban canyon” configuration (Oke 1987) in which the canyon geometry is described by building height ( $H$ ) and street width ( $W$ ). The model has been satisfactorily evaluated against measured fluxes and temperatures for several flux tower sites, performed well against other models in the International Urban Energy Balance Models Comparison Project, and produces known features of urban climatology, as discussed by Oleson (2012).

### 2.2 WRF model downscaling

WRF is a fully compressible conservative-form nonhydrostatic atmospheric model suitable for both research and weather prediction applications, which has demonstrated ability for resolving small-scale phenomena and clouds (Skamarock and Klemp 2008). A one-domain, 15-km WRF configuration over the U.S. and southern Canada is employed with 30 vertical levels from the surface to 10 hPa, including 7 levels in the lowest 1,000 m. WRF simulations are performed for two 20-year time slices for PD and MC periods. The PD simulation is based on observationally-based estimates of CO<sub>2</sub> and other GHGs during the industrial period, while the MC simulation, which is initialized at the end of the PD simulation in 2005, employs CO<sub>2</sub> and other GHG forcing based on phase five of the Coupled Model Intercomparison Project (CMIP5) RCP8.5 scenario (Moss et al. 2010). All simulations are performed for month-long intervals (e.g., cold-started at the beginning of each month).

Simulations are performed for all 12 months for the first four full years of each time slice, and for the 5 warmest months (May–September) for the subsequent 16 years (partial years are employed due to the high computational expense of the simulations). The initial and boundary conditions are provided by CCSM4 simulations run as part of CMIP5. Specific details on the WRF simulations can be found in Online Resource 2 (OR2). We compare the WRF-derived atmospheric forcing with CCSM4 climate simulations and also with the forcing dataset for phase 2 of the North American Land Data Assimilation System project (NLDAS-2) to provide some confidence in the WRF-derived forcing. The comparisons indicate that the WRF forcing appears to be a reasonable representation of CCSM4 climate at finer spatial resolution and compares favorably with NLDAS-2 climate (OR2).

Additionally, we compared the June–August diagnostic daily 2-m maximum and minimum temperature fields from the CLM4 output within CCSM4 (“CCSM4-CLM4”) and the offline simulations forced by WRF (“WRF-CLM4”) with 5,332 weather stations in the United States. Both the WRF-CLM4 and CCSM4-CLM4 fields provide reasonable depictions of daily temperature variability; WRF-CLM4 generally simulates daily minimum temperatures more accurately (i.e., with smaller biases) than CCSM4-CLM4, whereas the results are mixed for daily maximum temperatures as a result of regional downwelling long- and short wave radiation biases in WRF (OR2).

### 2.3 CLMU setup and simulations

A regional grid over the U.S. and southern Canada is established for CLM at a spatial resolution of  $1/8^\circ$  in latitude and longitude (Fig. 1). Surface data for the grid are derived following methods used in CLM4 global applications (Lawrence et al. 2011) (Fig. 1a). Urban fraction is aggregated from the 1 km data of Jackson et al. (2010) to the model grid (Fig. 1b). Urban properties are also provided by Jackson et al. (2010). These include thermal (e.g., thermal conductivity and heat capacity), radiative (e.g., albedo and emissivity), and morphological (e.g., H/W, roof fraction, average H, and pervious fraction of canyon floor) properties for each urban surface. For the model grid defined here, these properties are defined uniquely for nine geographic regions [see Fig. 3 in Jackson et al. (2010)] and three urban density classes (MD, HD, and TBD). In general, increasing urban density results in larger H/W, H, and roof fraction, and smaller pervious fraction, which we expect would increase urban temperature and the heat island (Oke et al. 1991).

In the current implementation of the urban model, only a single urban density type per grid cell is allowed. To examine the effects of the different urban density types on the UHI and measures of heat stress, separate simulations are conducted for MD, HD, and TBD. The three simulations are conducted for PD and MC, for a total of six simulations.

Two initial simulations using the MD PD and MC configurations are conducted to spin up model state variables by repeating the four full years of WRF forcing (1986–1989 and 2046–2049) ten times for a total of 40 years each. The state variables at the end of these two simulations are interpolated to the model state variables of the other surface datasets (HD and TBD) and the HD and TBD simulations are each run for an additional 8 years. All simulations are run for the available downscaled WRF atmospheric forcing for May–September. We focus here on analyzing the peak heat stress summer months (June, July, August).

### 2.4 Measures of heat stress and extreme heat events

Human thermal comfort, a subjective sensation, depends on environmental (ambient and radiant temperature, humidity, and air movement) and behavioral factors (metabolic rate and

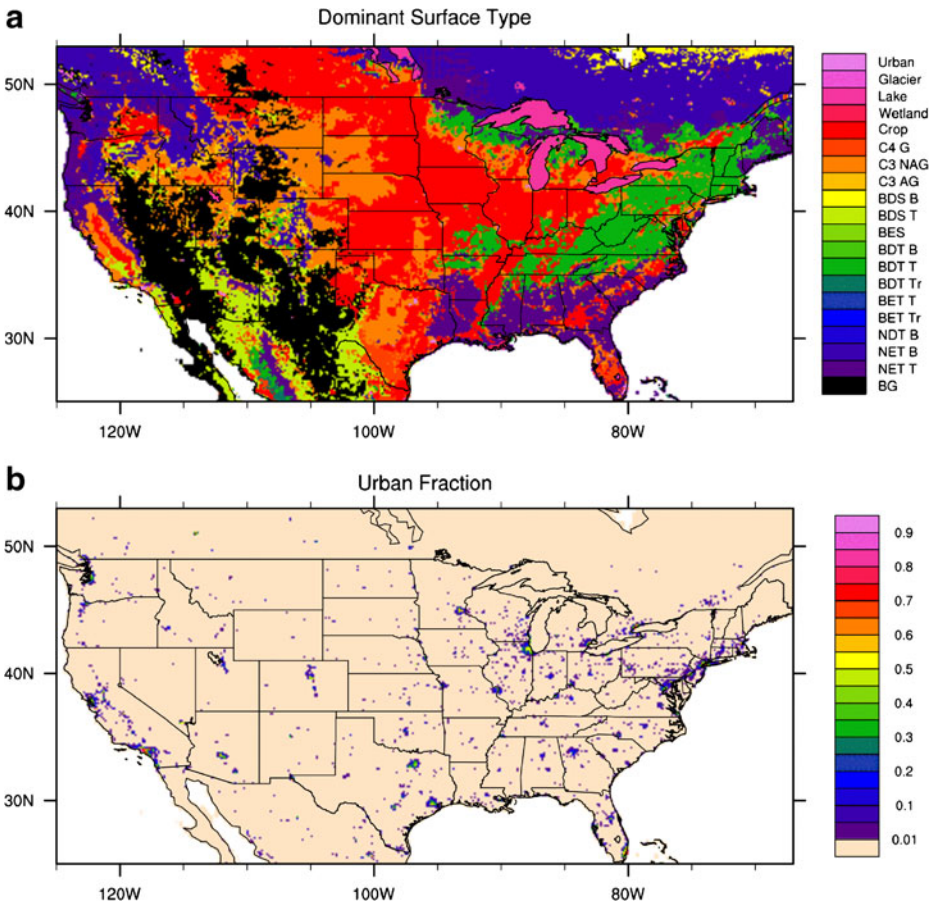


**Fig. 1** Model domain: **a**) dominant surface type by area, **b**) urban fraction of the grid cell. Spatial resolution is  $1/8^\circ$  in latitude and longitude. C4 G (C4 grassland), C3 NAG (C3 non-arctic grassland), C3 AG (C3 arctic grassland), BDS B (broadleaf deciduous shrub – boreal), BDS T (broadleaf deciduous shrub – temperate), BES (broadleaf evergreen shrub), BDT B (broadleaf deciduous tree – boreal), BDT T (broadleaf deciduous tree – temperate), BDT Tr (broadleaf deciduous tree – tropical), BET T (broadleaf evergreen tree – temperate), BET Tr (broadleaf evergreen tree – tropical), NDT B (needleleaf deciduous tree – boreal), NET B (needleleaf evergreen tree – boreal), NET T (needleleaf evergreen tree – temperate), BG (bare ground)

clothing) (Epstein and Moran 2006). Numerous indices have been developed to indicate thermal comfort and the heat stress experienced by an individual. Here, we focus on “direct indices” that are based on environmental variables and make assumptions about other environmental and behavioral factors. As in Fischer et al. (2012) we focus on two well-established environmental components of heat stress, temperature and humidity, but note that this may result in a conservative estimate of heat stress since radiation is not considered (Sherwood and Huber 2010). We implement five commonly used heat stress indices directly in the model (OR1). These are the National Weather Service (NWS) Heat Index (HI) (Rothfus 1990), Apparent Temperature (AT) (Steadman 1994), SWBGT (Willett and Sherwood 2012), Humidex (Masterson and Richardson 1979), and Discomfort Index (DI) (Epstein and Moran 2006). Heat indices are calculated for both rural (vegetation/soil) and urban areas.

The indices used here have different assumptions built into them and as such have limitations in terms of quantifying universally applicable levels of heat stress. The NWS HI for example assumes a 5'7" tall, 147 pound human wearing long trousers and a short-sleeved shirt walking outdoors in the shade at 3.1 miles per hour in a wind of 5 knots (Rothfus 1990). Furthermore, each index has its own unique thresholds to quantify different levels of heat stress. To provide some context for our results, we present a table of heat stress thresholds and associated categories for each index (see Table 3 as discussed in Section 3.2).

Extreme heat events are identified here following methods used in previous studies contrasting the response of rural and urban areas to climate change (Fischer et al. 2012; Oleson 2012). High heat stress days are defined as the number of days that the daily maximum air temperature exceeds the 95th percentile of the 1986–2005 rural daily maximum temperature. High heat stress nights are defined similarly using the daily minimum temperature. High heat stress days and nights are assessed using the five heat indices as well. We also quantify changes in heat stress categories for each index as mentioned above. Results are presented for four North American cities; Houston, Phoenix, Toronto, and New York. Houston has a humid subtropical climate characterized by a hot humid summer, while Phoenix has a subtropical desert climate with extremely hot and dry summers with occasional influxes of monsoonal moisture beginning in late July, thus providing contrasting aspects of heat stress. New York is the most populous city in the U.S. while the city of Toronto is actively involved in understanding and preparing for the effects of climate change on heat stress (Toronto Public Health 2011).

### 3 Results

#### 3.1 Dependence of present-day heat island and heat indices on urban density

Distinct differences in the urban-rural air temperature (UHI) and heat stress indices between urban density classes are evident for present day (Fig. 2). The UHI increases from an average of 1.3 °C for MD urban over the model domain to 1.7 °C and 3.2 °C for HD and TBD, respectively. This is mainly a consequence of larger H/W and smaller pervious fraction. Urban areas have lower relative humidity than rural areas, with the disparity increasing as urban density increases. Urban vapor pressure (VP) is generally lower than rural but is fairly constant across density classes, indicating that the lower relative humidity is caused mainly by warmer urban temperatures. As noted by Fischer et al. (2012) for the SWGBT, lower urban humidity offsets to some extent the higher urban temperature, however, there is still substantial urban amplification of heat stress. The HI and Humindex in general have higher values of heat stress for all density classes than the UHI alone despite lower urban humidity. The AT and DI are slightly lower than the UHI alone, but larger than the SWBGT (although note that the DI is specified in terms of units, not °C).

Figures 3 and 4 illustrate the average diurnal cycle of present day temperature, humidity, and the heat indices for two contrasting cities, Houston and Phoenix. For reference, observed June–August climatological maximum (Tmax) and minimum air temperature (Tmin) (at the respective major airports) is also shown at the times of model rural Tmax and Tmin (NOAA NCDC 2012). For Houston, the observed Tmax is warmer than the model rural Tmax but comparable with the model MD class temperature. The model rural Tmin compared to observations has a warm bias of 1.4 °C. For Phoenix, observed air temperature falls between the model rural and MD class temperatures, indicating that these are both reasonable simulations of air temperature.

In general, results are similar to the summertime averages shown in Fig. 2 with higher urban than rural temperature and lower humidity, the differences increasing with urban density, but

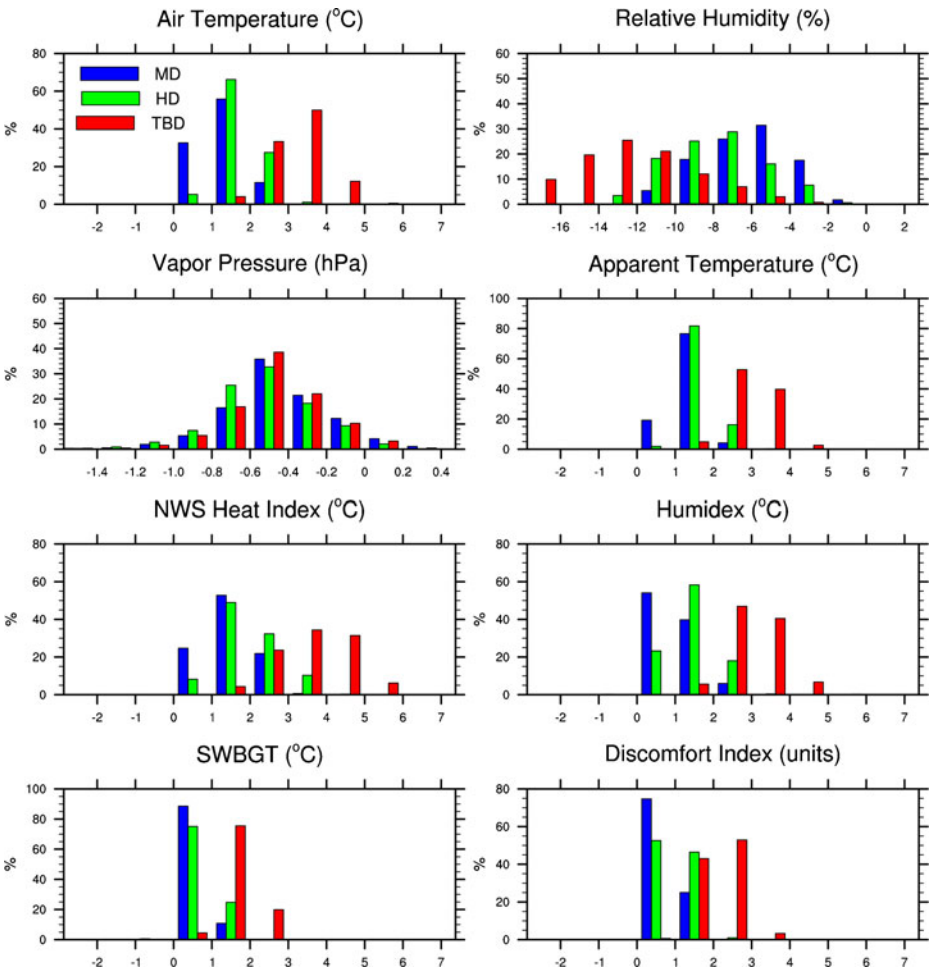


**Fig. 2** Barcharts of the summer (June–August) 1986–2005 climatology of urban minus rural 2-m air temperature, relative humidity, vapor pressure, and heat indices for urban medium density (MD), high density (HD), and tall building district (TBD) classes over the model domain shown in Fig. 1

this varies depending on city and time of day. For Houston, the maximum UHI occurs at night for all density classes (1.5 °C, 2.3 °C, and 4.2 °C, for MD, HD, and TBD, respectively). Peak daytime urban air temperatures are 1.2 °C, 1.6 °C, and 3.0 °C warmer than rural maximums and nighttime minimums are 0.9 °C, 1.9 °C, and 3.7 °C warmer than rural minimums (Table 1). In contrast to temperature, urban humidity (both relative humidity, and VP which is an absolute measure of humidity) is lowest during the day when it is most similar to rural humidity and highest at night when most dissimilar to rural humidity.

During both daytime and nighttime, although urban heat stress is higher than rural, the urban-rural contrast in heat stress indicated by the indices is generally less than indicated by temperature alone (Table 1). One exception is that during nighttime when relative humidity is highest, the urban-rural heat stress contrast as indicated by the HI in Houston is considerably amplified compared to air temperature alone. Nighttime minimums of urban HI for

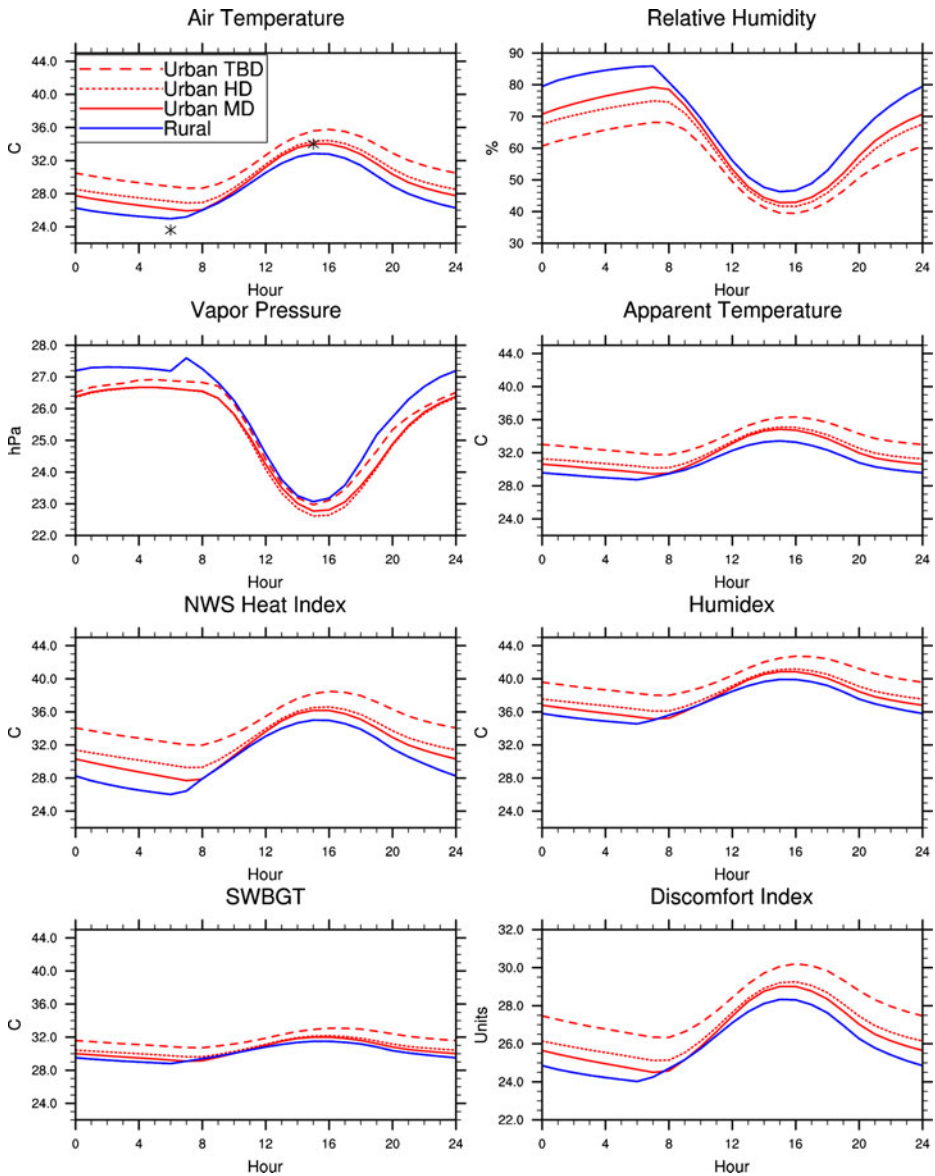


**Fig. 3** Average summer (June–August) 1986–2005 diurnal cycles of 2-m air temperature, relative humidity, vapor pressure, and heat indices for a region centered over Houston (29.52–30.02°N, 264.4–264.9°E). Also shown are climatological (1981–2010) daily maximum/minimum air temperature (asterisks) from the weather station at the Houston Bush Intercontinental Airport (GHCND:USW00012960; NOAA NCDC 2012), plotted at the time of maximum/minimum rural temperature

Houston are 1.7 °C, 3.3 °C, and 6.0 °C warmer than rural HI (compare to 0.9 °C, 1.9 °C, and 3.7 °C for temperature alone).

The urban and rural diurnal range in air temperature is much greater in Phoenix than Houston (e.g., the urban diurnal range is 14.5 °C and 7.8 °C for Phoenix and Houston, respectively), which is linked to the much lower humidity in Phoenix (VP=7–10 hPa) compared to Houston



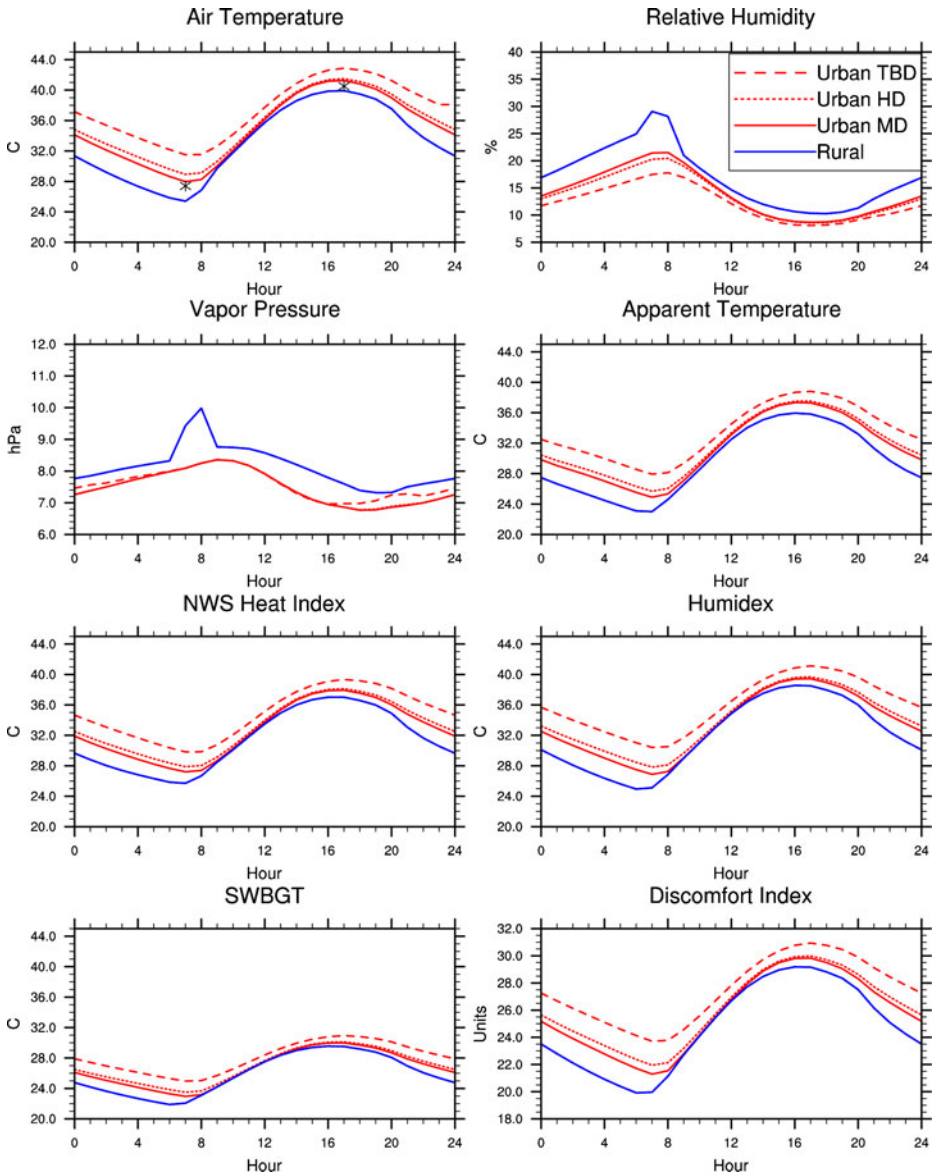


**Fig. 4** As in Fig. 3 but for a region centered over Phoenix (33.20–33.70°N, 247.68–248.18°E) Asterisks denote climatological (1981–2010) daily maximum/minimum air temperature from the weather station at the Phoenix International Airport (GHCND:USW00023183; NOAA NCDC 2012), plotted at the time of maximum/minimum rural temperature

(VP=23–27 hPa). Analysis of diurnal cycles of rural and urban energy balance show that this is due in part to more longwave radiation loss at night in Phoenix resulting in larger urban/rural cooling rates (not shown). The nighttime/daytime contrast in UHI is also larger for Phoenix with for example a nighttime UHI of 6.1 °C compared to 3.0 °C during daytime for the TBD class. Because of lower humidity, both the daytime and nighttime urban-rural contrast in heat

**Table 1** Summer (June–August) 1986–2005 climatology of daily maximum (Max) and minimum (Min) 2-m air temperatures and heat indices for Houston (29.52–30.02°N, 264.4–264.9°E) and Phoenix (33.2–33.7°N, 247.68–248.18°E) regions as shown in Figs. 3 and 4. AT (apparent temperature), HI (NWS heat index), SWBGT (simplified wet bulb globe temperature), DI (discomfort index)

	Houston							
	Max				Min			
	Rural	MD	HD	TBD	Rural	MD	HD	TBD
T (°C)	32.8	34.0	34.4	35.8	25.0	25.9	26.9	28.7
AT (°C)	33.4	34.8	35.1	36.3	28.7	29.4	30.2	31.8
HI (°C)	35.0	36.2	36.6	38.5	26.0	27.7	29.3	32.0
Humidex (°C)	39.9	40.9	41.2	42.7	34.5	35.1	36.1	38.0
SWBGT (°C)	31.5	32.0	32.2	33.1	28.8	29.1	29.6	30.7
DI (units)	28.3	29.0	29.3	30.2	24.0	24.5	25.1	26.3
	Phoenix							
T (°C)	39.9	41.2	41.5	42.9	25.4	28.0	28.9	31.5
AT (°C)	35.9	37.3	37.5	38.8	23.0	24.9	25.7	27.9
HI (°C)	37.0	37.9	38.1	39.3	25.7	27.2	27.9	29.8
Humidex (°C)	38.6	39.4	39.7	41.1	24.9	26.9	27.8	30.4
SWBGT (°C)	29.5	30.0	30.1	30.9	21.9	23.0	23.5	25.0
DI (units)	29.2	29.8	30.0	30.9	19.9	21.3	21.9	23.7

stress is always lower than the contrast in air temperature. This is a direct consequence of the heat index formulations for lower humidity (see OR1, Fig. S1). For example, the peak daytime urban HI is 0.9 °C, 1.1 °C, and 2.3 °C warmer than rural HI, while the UHI is 1.3 °C, 1.6 °C, and 3.0 °C, for MD, HD, and TBD, respectively (Table 1). Similarly, the nighttime urban HI is 1.5 °C, 2.2 °C, and 4.1 °C warmer than the rural HI, compared to 2.6 °C, 3.5 °C, and 6.1 °C for the UHI.

### 3.2 Future changes in urban temperature and heat stress

Table 2 indicates that future urban temperatures at the local scale are somewhat influenced by urban density. In particular, while the MD and HD urban temperatures respond similarly to climate change, there is a small shift in the distribution of TBD temperatures to warmer conditions (by about 0.1 °C; Table 2). The changes in urban heat stress as indicated by the AT, HI, and Humidex heat indices are amplified compared to just temperature alone (Table 2). Urban heat stress indicated by these indices is 0.5–1.0 °C above the increase in temperature depending on density class and heat index. The maximum values of heat stress are higher as well, with maximum increases of 4.1 °C, 4.8 °C, and 4.7 °C for AT, HI, and Humidex, respectively, compared to a maximum of 3.6 °C for temperature alone. The distribution of higher values generally occurs in more humid regions such as the Eastern U.S. (not shown).

The frequency of high heat stress days and nights for New York, Phoenix, Toronto, and Houston is shown in Fig. 5. Select results for the MD class are shown for temperature alone (Fig. 5a–d) and the HI (Fig. 5e–h), but full results for all density classes and heat indices are tabulated in Online Resource 3 (OR3, Tables S1–S4). The HI is chosen because it is the most non-linear index in accounting for humidity (OR1, Fig. S1) and because it is the standard index used by the U.S. National Weather Service.

**Table 2** Changes (2046–2065 minus 1986–2005) in summer (June–August) climatology of urban 2-m air temperature (T), relative humidity (RH), vapor pressure (VP) and heat indices averaged over the model domain shown in Fig. 1. All changes are significant using a Student's *t*-test at a significance level of  $\alpha=0.05$ 

	T (°C)	RH (%)	VP (hPa)	AT (°C)	HI (°C)	Humidex (°C)	SWBGT (°C)	DI (units)
MD	2.22	-1.5	1.9	2.84	2.74	3.23	1.97	1.94
HD	2.23	-1.5	1.9	2.84	2.76	3.23	1.97	1.94
TBD	2.31	-1.5	1.9	2.92	2.92	3.32	2.02	1.98

When temperature is used as an indicator of present day heat stress, high heat stress days and nights occur more frequently in urban than rural areas (Fig. 5a–d). Urban high heat stress occurs more frequently at night, a consequence of the daytime/nighttime asymmetry in the UHI. For example, for present day in Houston there are 32 nights for which the urban  $T_{min}$  is above 27 °C (the 95th percentile rural  $T_{min}$ ; OR3, Table S4), while there are 20 days where urban  $T_{max}$  is above 37 °C (the 95th percentile rural  $T_{max}$ ; OR3, Table S4). In general, Houston has the largest day and night urban amplification of heat stress for present day followed by Phoenix. Increasing urban density increases the number of high heat stress days and nights. For example, the TBD class for Houston has 84 nights (91 % of summer nights) where urban  $T_{min}$  is above 27 °C and 50 days (54 % of summer days) where urban  $T_{max}$  is above 37 °C (OR3, Table S4).

As expected from previous analysis (Diffenbaugh and Ashfaq 2010; Oleson 2012; Fischer et al. 2012), climate change increases the number of high heat stress days and nights in both rural and urban areas (Fig. 5a–d). Rural high heat stress days and nights increase substantially by 200–860 %. Rural Houston in particular has 48 high heat stress nights due to climate change, more than half of summer nights. On the other hand, the exceedance frequency for urban areas is particularly high in Phoenix, Toronto, and Houston, which have the largest urban amplification of high heat stress days/nights at present day. Houston, for example, has 78 nights with urban  $T_{min}$  above 27 °C and 53 days with urban  $T_{max}$  above 37 °C for the MD class. Increasing urban density increases the number of high heat stress days and nights under climate change as well. The magnitude of this increase appears to be limited by how high the urban exceedance frequency is for present day. For example, the number of high heat stress nights in Houston increases from 78 for MD to 90 for TBD (OR3, Table S4), while in New York the number of nights nearly doubles from 32 to 62 (OR3, Table S1).

In general, urban amplification of high heat stress days and nights for present day using the HI is about the same or less than if temperature alone is used (Fig. 5e–h). Presumably this is in part because any increased heat stress due to humidity in the HI is already reflected in the 95th percentile rural values. For instance, in the relatively dry city of Phoenix, the number of urban heat stress days/nights actually decreases from 16/26 days using temperature alone to 12/20 days using the HI. The exception is urban high heat stress nights in Toronto, which increases from 18 nights using temperature alone to 31 nights using the HI.

Similarly, climate change effects on urban heat stress as indicated by the HI are similar to those using temperature alone, differing by less than 5 days in most cases. Two exceptions are noteworthy; urban high heat stress nights for Toronto increase from 46 using temperature alone to 60 nights as indicated by the HI, and urban high heat stress days for Houston increase from 53 to 77 days. Note that the error bars in Fig. 5 indicate that the changes (MC minus PD) in rural and urban high heat stress days and nights as indicated by temperature and the HI are all significant at a significance level of  $\alpha=0.05$ .

As noted in Section 2.4, the different assumptions and limitations of each heat index can make it difficult to assess the potential impact of changes in heat stress on humans. The

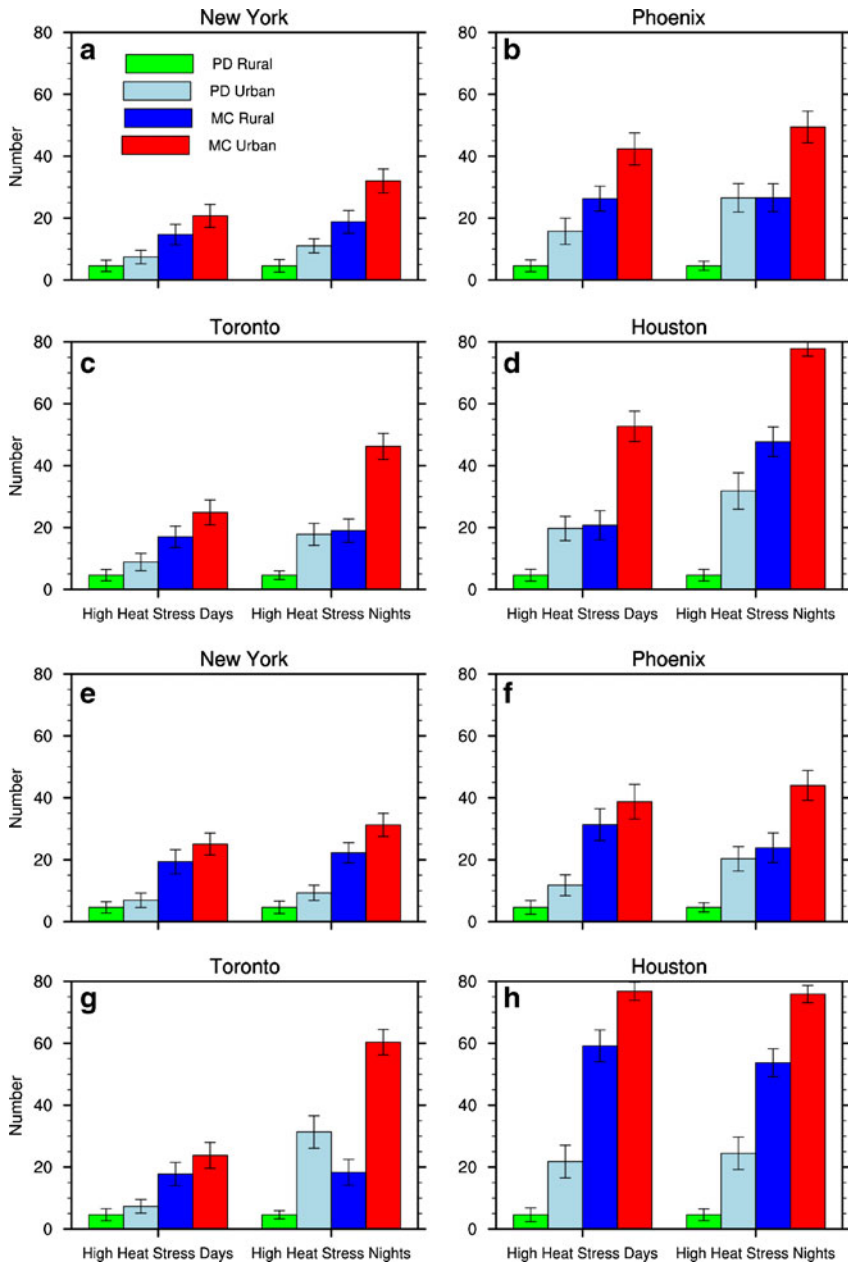


**Fig. 5** Average summer (June–August) frequency of urban and rural high heat stress days and nights for the cities of New York, Phoenix, Toronto, and Houston, determined from (a–d) 2-m air temperature and (e–h) the NWS Heat Index (HI). Urban results are for the MD class. High heat stress days are defined as the number of days that the daily maximum air temperature/HI exceeds the 95th percentile of the 1986–2005 rural daily maximum air temperature/HI. High heat stress nights are defined similarly using the daily minimum air temperature/HI. PD (present-day; 1986–2005), MC (mid-century; 2046–2065). Error bars denote the sampling uncertainty, i.e., the 95 % confidence interval around the mean estimate based on the Student's  $t$  distribution. They do not represent any other sources of uncertainties, e.g., model structural or parameterization uncertainties (Fischer et al. 2012)

application of thresholds to define categories of heat stress for each index is one method of providing a qualitative assessment that is perhaps more appealing to city planners and the general population (Table 3 for Houston and Tables S5–S7 in OR3 for New York, Phoenix, and Toronto). However, note that the alignment of columns in these tables does not mean to imply equality between different categories (e.g., the “very hot” category of the AT is not necessarily equivalent to the “danger” category of the HI). Regardless, Table 3 is clear evidence that heat stress is projected here to increase by mid-century in both rural and urban areas no matter how it is determined. There is a clear shift from lower to higher categories of heat stress for all indices. For example, the number of days in the AT “extremely hot” category increases by 37 days for rural and 48 days for urban. As indicated by the SWBGT, there are 14 more days in the “extreme” category for rural, and 30 more days for urban. There is also on average 1 day per four summers that falls in the HI “extreme danger” category and 1 day per 5 summers that falls in the Humidex “imminent heat stroke” category for urban.

#### 4 Conclusions

The objectives of this study are to quantify the UHI and urban/rural heat stress for present-day (PD), quantify changes in urban/rural heat stress for an RCP8.5 projection of mid-21st century climate (MC), and examine the effects of urban density (MD, HD, and TBD) on urban heat stress for boreal summer over the U.S and southern Canada. Numerical simulations are conducted using CLM coupled to the urban canyon model CLMU. Five commonly used heat stress indices combining temperature and humidity effects are implemented in CLM. Results are analyzed in terms of summer mean, daytime maximum and nighttime minimum climatology, and high heat stress days and nights with a focus on the climates of New York, Phoenix, Toronto, and Houston. The primary findings of this study are as follows:

- The domain-wide PD UHI increases from an average of 1.3 °C for the MD class over the model domain to 1.7 °C and 3.2 °C for HD and TBD, respectively. Urban areas have lower relative humidity than rural areas, with the disparity increasing as urban density increases.
- The domain-wide PD urban-rural contrast in heat stress differs according to the heat stress index used. The HI and Humidex in general have higher urban-rural heat stress for all density classes than defined by temperature alone. The DI and AT indices have slightly lower urban-rural heat stress than temperature alone, but larger than the SWBGT.
- Analysis of the diurnal cycle for Houston and Phoenix indicates (in contrast to the domain-wide results) although PD urban heat stress is higher overall than rural, the urban-rural contrast in heat stress as indicated by the heat indices is generally similar to or less than indicated by temperature alone. An exception is noted for the HI in Houston at night, where the nighttime minimums of urban HI are 0.8 °C to 2.3 °C warmer than temperature alone depending on density class.
- Future urban temperatures at the local scale over the model domain are somewhat influenced by urban density. The MD and HD urban temperatures respond similarly to climate change, while TBD temperatures increase by an additional 0.1 °C compared to MD and HD. Future urban heat stress as indicated by the AT, HI, and Humidex is amplified by 0.5–1.0 °C compared to temperature alone.
- Climate change increases the number of high heat stress days and nights in both rural and urban areas for the four cities, the number being highly dependent on heat stress index, urban density, and each city’s climatic setting. The results for Houston are notable for large increases

**Table 3** Average number of summer (JJA) days in each heat stress index category for present-day (PD; 1986–2005) and mid-21st century (MC; 2046–2065) rural and urban for the city of Houston. Urban results are for the MD class. Categories and thresholds for 2-m air temperature, apparent temperature, and NWS heat index are from Smith et al. (2013), Humidex from Masterson and Richardson (1979), simplified wet bulb globe temperature from Willett and Sherwood (2012), discomfort index from Epstein and Moran (2006). The 85th, 90th, and 95th percentiles for 2-m air temperature and apparent temperature are calculated from PD rural and applied to both rural and urban results

2-m Air Temperature					
Category	Hot	Very Hot	Extremely Hot		
Threshold	>85th percentile	> 90th percentile	> 95th percentile		
PD Rural	4.60	4.60	4.60		
MC Rural	10.05	12.85	20.75		
PD Urban	7.30	11.55	19.70		
MC Urban	5.45	10.80	52.70		
Apparent Temperature					
PD Rural	4.60	4.60	4.60		
MC Rural	8.85	13.60	41.30		
PD Urban	8.05	11.80	22.25		
MC Urban	3.95	6.60	70.60		
NWS Heat Index					
Category	Caution	Danger	Extreme Danger		
Threshold	>80 °F (26.7 °C)	>105 °F (40.6 °C)	>130 °F (54.4 °C)		
PD Rural	7.40	0.45	0.00		
MC Rural	1.90	21.85	0.00		
PD Urban	4.85	5.30	0.00		
MC Urban	1.20	52.15	0.25		
Humidex					
Category	Some Discomfort	Dangerous	Imminent Heat Stroke		
Threshold	≥30 °C	>46 °C	≥54 °C		
PD Rural	28.20	0.20	0.00		
MC Rural	5.85	7.05	0.00		

**Table 3** (continued)

PD Urban	15.80	73.25	2.50	0.00
MC Urban	4.00	60.35	27.45	0.20
Category	Simplified Wet Bulb Globe Temperature			
Threshold	–	High	Very High	Extreme
PD Rural	–	>28 °C	>32 °C	>35 °C
MC Rural	–	39.25	48.55	0.70
PD Urban	–	6.05	70.25	14.65
MC Urban	–	23.20	61.80	3.90
	–	4.80	52.55	34.00
Category	Discomfort Index			
Threshold	No Heat Stress	Mild Sensation of Heat	Moderately Heavy Heat Load	Severe Heat Load
PD Rural	<22 units	≥22 units	>24 units	>28 units
MC Rural	0.30	1.55	18.35	71.80
PD Urban	0.00	0.20	4.40	87.40
MC Urban	0.20	1.15	10.10	80.55
	0.00	0.10	2.85	89.05

in high heat stress nights, with more than half of summer nights qualifying as high HS in not only urban areas but rural areas as well. This indicates a need to consider adaptive capacity and vulnerability of both rural and urban populations in the context of climate change.

These results should be considered to be qualitative in light of the limitations of the numerical modeling performed here, particularly the results presented for specific cities. These limitations include the offline nature of the modeling thus not capturing potential land-atmosphere feedbacks, the inadequacies of the urban canyon model in representing complex urban surfaces both within a city and between cities, the accuracy with which the atmospheric forcing is reproduced by WRF for present day and projected for mid-century, and that it was only computationally feasible to downscale one GCM realization. Other important questions not addressed here because of space limitations are how urban areas will change to accommodate overall growth in population and the projected increase in urban dwellers and how this will affect and interact with the climate and heat stress in cities. We plan to address this in future work. However, the current study emphasizes the important effects of urban areas and urban density on the amplification of heat stress both now and in the future.

**Acknowledgments** This research was supported in part by NASA grant NNX10AK79G (the SIMMER project). K.W. Oleson acknowledges support from the NCAR WCIASP. NCAR is sponsored by the NSF.

## References

- CDC (Centers for Disease Control) (2006) Heat-related Deaths—United States, 1999–2003, Mortality and Morbidity Weekly Report published by the Centers for Disease Control, July 28, 2006/55(29):796–798 <http://www.cdc.gov/mmwr/preview/mmwrhtml/mm5529a2.htm>
- Conti S, Meli P, Minelli G et al (2005) Epidemiologic study of mortality during the summer 2003 heat wave in Italy. *Environ Res* 98:390–399
- Delworth T, Mahlman J, Knutson T (1999) Changes in heat index associated with CO<sub>2</sub>-induced global warming. *Clim Change* 43:369–386
- Diffenbaugh NS, Ashfaq M (2010) Intensification of hot extremes in the United States. *Geophys Res Lett* 37, L15701. doi:10.1029/2010GL043888
- Epstein Y, Moran DS (2006) Thermal comfort and the heat stress indices. *Ind Health* 44:388–398
- Fischer EM, Oleson KW, Lawrence DM (2012) Contrasting urban and rural heat stress responses to climate change. *Geophys Res Lett* 39, L03705. doi:10.1029/2011GL050576
- Gent PR, Danabasoglu G, Donner LJ et al (2011) The Community Climate System Model version 4. *J Climate* 24:4973–4991
- IPCC (2007) In: Solomon S, Qin D, Manning M, Chen Z, Marquis M, Averyt KB, Tignor M, Miller HL (eds) *Climate Change 2007: The Physical Science Basis. Contribution of Working Group I to the Fourth Assessment Report of the Intergovernmental Panel on Climate Change*. Cambridge University Press, Cambridge, 996 pp
- Jackson TL, Feddema JJ, Oleson KW et al (2010) Parameterization of urban characteristics for global climate modeling. *A Assoc Am Geog* 100:848–865
- Lawrence DM, Oleson KW, Flanner MG et al (2011) Parameterization improvements and functional and structural advances in version 4 of the Community Land Model. *J Adv Model Earth Syst* 3, M03001. doi:10.1029/2011MS000045
- Masterson J, Richardson F (1979) Humidex, a method of quantifying human discomfort due to excessive heat and humidity. CLI 1-79, Environment Canada, Atmospheric Environment Service, Downsview, Ontario
- Meehl GA, Tebaldi C (2004) More intense, more frequent, and longer lasting heat waves in the 21st century. *Science* 305:994–997
- Moss RH, Edmonds JA, Hibbard KA (2010) The next generation of scenarios for climate change research and assessment. *Nature* 463:747–756
- NOAA NCDC (2012) National Oceanic and Atmospheric Administration, National Climatic Data Center. <http://www.ncdc.noaa.gov/oa/ncdc.html>. Accessed 10 December 2012



- Oke TR (1987) *Boundary Layer Climates*. 2nd ed, Routledge
- Oke TR, Johnson GT, Steyn DG et al (1991) Simulation of surface urban heat islands under “ideal” conditions at night, part 2: diagnosis of causation. *Bound-Layer Meteor* 56:339–358
- Oleson KW, Bonan GB, Feddema J et al (2008) An urban parameterization for a global climate model. 1. Formulation and evaluation for two cities. *J Appl Meteorol Clim* 47:1038–1060
- Oleson KW (2012) Contrasts between urban and rural climate in CCSM4 CMIP5 climate change scenarios. *J Climate* 25:1390–1412
- Rogot E, Sorlie PD, Backlund E (1992) Air-conditioning and mortality in hot weather. *Am J Epidemiol* 136:106–116
- Rothfus LP (1990) The Heat Index “Equation” (or, more than you ever wanted to know about heat index). Scientific Services Division, NWS Southern Region Headquarters, Fort Worth, TX
- Sailor DJ (2010) A review of methods for estimating anthropogenic heat and moisture emissions in the urban environment. *Int J Climatol* 31:189–199
- Sherwood SC, Huber M (2010) An adaptability limit to climate change due to heat stress. *Proc Nat Acad Sci* 107:9552–9555
- Skamarock WC, Klemp JB (2008) A time-split non-hydrostatic atmospheric model for weather research and forecasting applications. *J Comput Phys* 227:3465–3485
- Smith TT, Zaitchik BF, Gohlke JM (2013) Heat waves in the United States: definitions, patterns and trends. *Clim Change* 118:811–825
- Steadman RG (1994) Norms of apparent temperature in Australia. *Aust Met Mag* 43:1–16
- Stone B (2012) *The city and the coming climate: Climate change in the places we live*. Cambridge University Press, New York
- Toronto Public Health (2011) Protecting vulnerable people from health impacts of extreme heat. Toronto, Ontario, 44pp. <http://www.toronto.ca/health/hpche>
- Uejio CK, Wilhelmi OV, Golden JS et al (2011) Intra-urban societal vulnerability to extreme heat: the role of heat exposure and the built environment, socioeconomic, and neighborhood stability. *Heath Place* 17:498–507
- Willett KM, Sherwood S (2012) Exceedance of heat index thresholds for 15 regions under a warming climate using the wet-bulb globe temperature. *Int J Climatol* 32:161–177